Upper ocean manifestations of a reducing meridional overturning circulation

M. D. Thomas,[1] A. M. de Boer,[2] D. P. Stevens,[3] and H. L. Johnson[4]

[1] Most climate models predict a slowing down of the Atlantic Meridional Overturning Circulation during the 21st century. Using a 100 year climate change integration of a high resolution coupled climate model, we show that a 5.3 Sv reduction in the deep southward transport in the subtropical North Atlantic is balanced solely by a weakening of the northward surface western boundary current, and not by an increase in the southward transport integrated across the interior ocean away from the western boundary. This is consistent with Sverdrup balance holding to a good approximation outside of the western boundary region on decadal time scales, and may help to spatially constrain past and future change in the overturning circulation. The subtropical gyre weakens by 3.4 Sv over the same period due to a weakened wind stress curl. These changes combine to give a net 8.7 Sv reduction in upper western boundary transport. **Citation:** Thomas, M. D., A. M. de Boer, D. P. Stevens, and H. L. Johnson (2012), Upper ocean manifestations of a reducing meridional overturning circulation, *Geophys. Res. Lett.*, *39*, L16609, doi:10.1029/2012GL052702.

1. Introduction

[2] The northward heat flux associated with the Atlantic Meridional Overturning Circulation (AMOC) is an important part of the climate system, and contributes to the relatively warm temperatures of north west Europe. Climate simulations of the remainder of the twenty first century suggest that growing quantities of atmospheric carbon dioxide will cause a reduction in the strength of the AMOC [e.g., *Intergovernmental Panel on Climate Change*, 2007]. So far observations have not seen any conclusive evidence for a weaker AMOC. Hydrographic sections at 25°N suggested that the AMOC decreased by 30% between the years 1957–2004 [*Bryden et al.*, 2005] but the interpretation has been called into question [*Searl et al.*, 2007; *Wunsch and Heimbach*, 2006] because it does not account for the strong sub-annual variability of the AMOC [*Kanzow et al.*, 2007; *Cunningham et al.*, 2007]. A synthesis of hydrographic data across the whole North Atlantic does indicate a small and significant decrease in the AMOC in the subtropics but also a small increase in the AMOC in the subpolar region [*Lozier et al.*, 2010]. While progress has been made in understanding the time and spatial variability of the AMOC, there is currently no clear understanding of the zonal expression of a potential reduction in the subtropical AMOC.

[3] Sverdrup theory [*Sverdrup*, 1947] relates the time mean depth-integrated circulation in the upper ocean to the curl of the wind stress. In the subtropics Sverdrup theory is believed to hold to a good order of approximation in the interior (east of the western boundary current), where the ocean is in linear vorticity balance and there is a presumed level of no motion. The extent to which the wind field determines the flow in the interior will control how much the interior ocean can adjust to a change in the southwards deep ocean transport. If Sverdrup balance holds perfectly and the winds do not change, all adjustment needs to occur in the northward flowing surface western boundary current. It is non trivial to test the validity of Sverdrup balance in the ocean because the ocean takes a few years to reach this balance [*Anderson and Killworth*, 1977]. At these time scales there are a limited number of interior ocean observations and there are often considerable differences between the available wind stress products [*Josey et al.*, 2002]. Recent analysis based on a state estimation product, which combines observations in a dynamical model, suggests that Sverdrup balance may indeed hold to first order on decadal time scales over large parts of the subtropical gyre [*Wunsch*, 2011]. However, how Sverdrup balance might change in a warmer climate and its constraint on future change in the AMOC have yet to be established. Understanding the structure of changes in meridional overturning over various time scales may provide useful insight for the development of future ocean monitoring strategies.

[4] The aim of this paper is to address the question of how a change in the AMOC will manifest itself in the subtropical North Atlantic. Using an idealised climate projection experiment in the high resolution coupled climate model HiGEM, we establish how upper ocean meridional transport will change when the southwards deep transport weakens, and we determine whether the changes are consistent with Sverdrup balance.

2. Model Description

[5] The data used in this study are from the coupled climate model, HiGEM [*Roberts et al.*, 2009; *Shaffrey et al.*, 2009], which is based on the Met Office HadGEM1 model [*Johns et al.*, 2006] but has a higher spatial resolution. It uses a spherical latitude-longitude grid between 90°S and 90°N with a horizontal resolution of 0.83° latitude × 1° longitude in the atmosphere and an eddy permitting 1/3° × 1/3° resolution ocean. The increase in ocean grid resolution relative to HadGEM1 allows for a better representation of

[1]School of Environmental Sciences, University of East Anglia, Norwich, UK.
[2]Department of Geological Sciences, Stockholm University, Stockholm, Sweden.
[3]School of Mathematics, University of East Anglia, Norwich, UK.
[4]Department of Earth Sciences, University of Oxford, Oxford, UK.

Corresponding author: M. D. Thomas, School of Environmental Sciences, University of East Anglia, Norwich NR4 7TJ, UK. (matthew.thomas@uea.ac.uk)
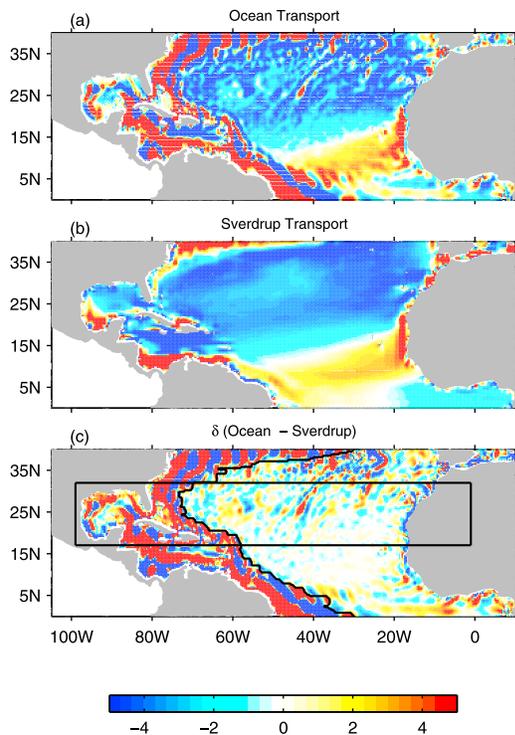
Figure 1. North Atlantic transport terms from equation (1), averaged over the first 10 years of the Control run: (a) meridional ocean transport depth-integrated from the surface to 1500 m, (b) Sverdrup transport derived from the wind field and (c) residual (the difference between Figures 1b and 1a). The box in Figure 1c outlines the region of focus throughout this study and the black line separates the interior ocean and western boundary domains, as defined in the text. Units are $m^2 s^{-1}$.

topographic straits and improvements have been noted in the transport through, for example, the Fram Strait, the Denmark Strait and the Bering Strait [*Shaffrey et al.*, 2009]. The ocean component has 40 vertical levels and the atmosphere component has 38 vertical levels, each with uneven spacing to allow higher boundary layer resolution. The ocean and atmosphere initial conditions are taken from the World Ocean Atlas 2001 and ECMWF analysis, respectively.

[6] Annual mean output from two simulations is used. The first is a 150 year control integration in which greenhouse gases are kept constant at present day concentrations. Hereafter this integration is labelled Control. The second simulation is a 100 year integration that is initiated from the Control integration at year 30. The atmospheric concentration of CO_2 is increased by 2% per year for the first 70 years until levels reach 4 times starting values and is then stabilised for the remaining 30 years. Henceforth this run will be labelled $2\%CO_2$. As we are not concerned with the initial 30 years, year 1 refers in each case to the first year after that period. Despite the relatively short 30 year spin up time, AMOC drift in the control run is small at 0.004 Sv year^{-1}.

3. Sverdrup Balance in the Subtropical Ocean

[7] Here we assess how well Sverdrup balance holds in the North Atlantic and whether the balance is affected by climate change. The degree to which the ocean is in

Sverdrup balance will affect how the meridional transport in the subtropical ocean will change as the AMOC weakens (assessed in section 4).

[8] Sverdrup balance refers to the balance between vorticity input to the ocean by the wind and advection of planetary vorticity in the ocean interior. It is derived from the depth integrated vorticity equation,

$$V = \frac{(\nabla \times \tau)_z}{\rho_0 \beta} + \delta, \qquad (1)$$

where Sverdrup balance is the balance between the first two terms and is the depth integral of the linear vorticity terms. Here V is the depth integrated meridional transport (integrated from the surface to some assumed mid-depth level of no vertical motion), τ is the wind stress, $(\nabla \times \tau)_z$ is the vertical component of the wind stress curl, β is the meridional gradient of the Coriolis frequency, ρ_0 is a reference density and δ is the residual. Henceforth V is referred to as the ocean transport and the first term on the right of (1) is referred to as the Sverdrup transport.

[9] The ocean comes into Sverdrup balance with the wind forcing by the propagation of baroclinic Rossby waves [*Anderson and Killworth*, 1977] which limit the transport to the thermocline and isolate it from the bottom topography. To allow for the adjustment period, an averaging time scale of 10 years is applied to all analysis of the Sverdrup balance in this study. This period is considered long enough to allow Rossby wave adjustment at any subtropical latitude [*Gill*, 1982].

[10] Figure 1 shows an example of Sverdrup balance in the Control scenario. Each term in equation (1) is time-averaged over the first 10 years. Note that the 10 year Sverdrup balance is similar to that achieved from longer averaging times of e.g. 30 years. The ocean transport is depth-integrated to 1500 m. Although there exist large transports in the deep ocean associated with topography that would cause significant departures from Sverdrup balance if equation (1) were to be depth integrated to the bottom, it has been verified that 1500 m lies consistently below the bulk of the upper ocean transport (but not so deep that it impinges greatly on the deep currents). Equivalent maps for the $2\%CO_2$ scenario are not shown since they differ only slightly. Sverdrup balance holds very well in the interior of the ocean under these simple assumptions when considered over scales larger than a few degrees. Small scale features in the ocean transport are not reproduced in the Sverdrup transport, in particular over parts of the Mid-Atlantic Ridge. Close to the western boundary and at latitudes greater than approximately 35°N Sverdrup balance breaks down entirely. The western boundary break down occurs generally within about 700 km of the coast, but in some regions the break down extends as far as 1000 km from the coast. Deviations from Sverdrup balance arise due to failings in the assumptions that the ocean is in linear vorticity balance and that there is a level of no vertical motion at 1500 m.

[11] We henceforth split the ocean into two domains which we define as an interior ocean domain that is in Sverdrup balance and a western boundary domain where Sverdrup balance breaks down. The black line in Figure 1c delineates the boundary between the two domains and is chosen as the line where the residual exceeds 5 $m^2 s^{-1}$ (note that outliers are removed to allow for a continuous contour).
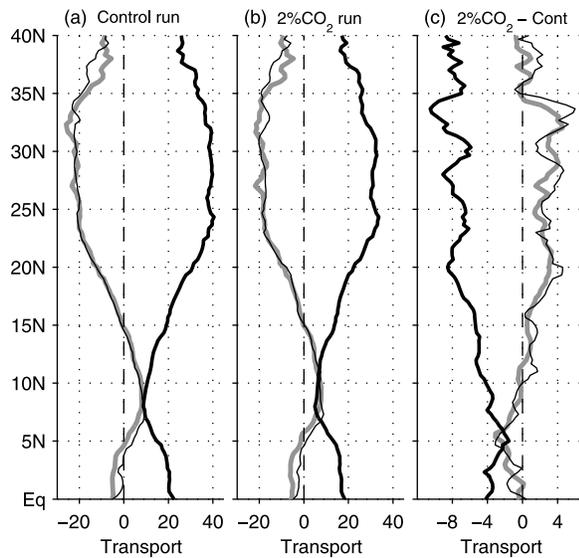
Figure 2. Decadal mean (years 70 to 80) North Atlantic zonally integrated Sverdrup transport (bold grey line), interior ocean transport (thin black line) and western boundary transport (bold black line) versus latitude. Transports are shown for (a) the Control run, (b) 2%CO_2 run and (c) the difference (2%CO_2 minus Control). The dashed vertical line marks zero transport. Units are Sverdrups (Sv; 10^6 m^{3}s^{-1}).

[12] Of primary interest in the context of a changing AMOC is the zonally integrated Sverdrup balance. To assess differences in the Sverdrup interior transport between the Control and 2%CO_2 scenarios, zonally integrated decadal mean transports (depth-integrated to 1500 m) are calculated for the years 70–80, a period after the point at which atmospheric CO_2 has stopped increasing. Figure 2 shows the ocean transport and Sverdrup transport in the interior for each scenario at each latitude between the equator and 40°N. Zonally integrated Sverdrup balance holds very well in the subtropics for both the Control and 2%CO_2 scenarios. This indicates that zonally integrated Sverdrup balance holds to first order throughout a changing climate, and that the small scale interior residuals evident in Figure 1c tend to cancel out once zonally integrated. No trend, significant at the 95% level, was found in either the (domain averaged) pointwise or zonally-integrated residual, δ, in the Control or 2%CO_2 scenarios. The time averages of the zonally-integrated residual in the Control and 2%CO_2 scenarios are respectively 1.1 Sv and 0.9 Sv when meridionally averaged between 17°N and 32°N. (Significance was tested using a block bootstrapping method that accounts for autocorrelation).

[13] The zonally integrated interior ocean transport is weaker throughout the subtropical gyre in the 2%CO_2 experiment and this is consistent with a weakened Sverdrup transport relative to the control (Figure 2). This decrease in zonally-integrated meridional transport by up to 6 Sv in the interior takes place at all latitudes in the subtropical North Atlantic (Figure 2c).

4. Transport Trends

[14] Here we analyse how the upper western boundary current, the upper ocean interior transport, and the deep southward transport combine to give a decreasing AMOC

trend in the 2%CO_2 run. The AMOC at 27°N (defined as the maximum overturning stream-function between depths 500 m and 2500 m) reduces from approximately 21 Sv to 15 Sv between years 1 and 70 whilst CO_2 levels are increasing, and then stabilises once CO_2 is kept constant (Figure 3a). Throughout this section, unless stated otherwise, transport values refer to the annual mean, meridionally averaged, zonally integrated, transport within the domains shown in Figure 1c. The meridional averaging provides an overall picture of the meridional overturning trends instead
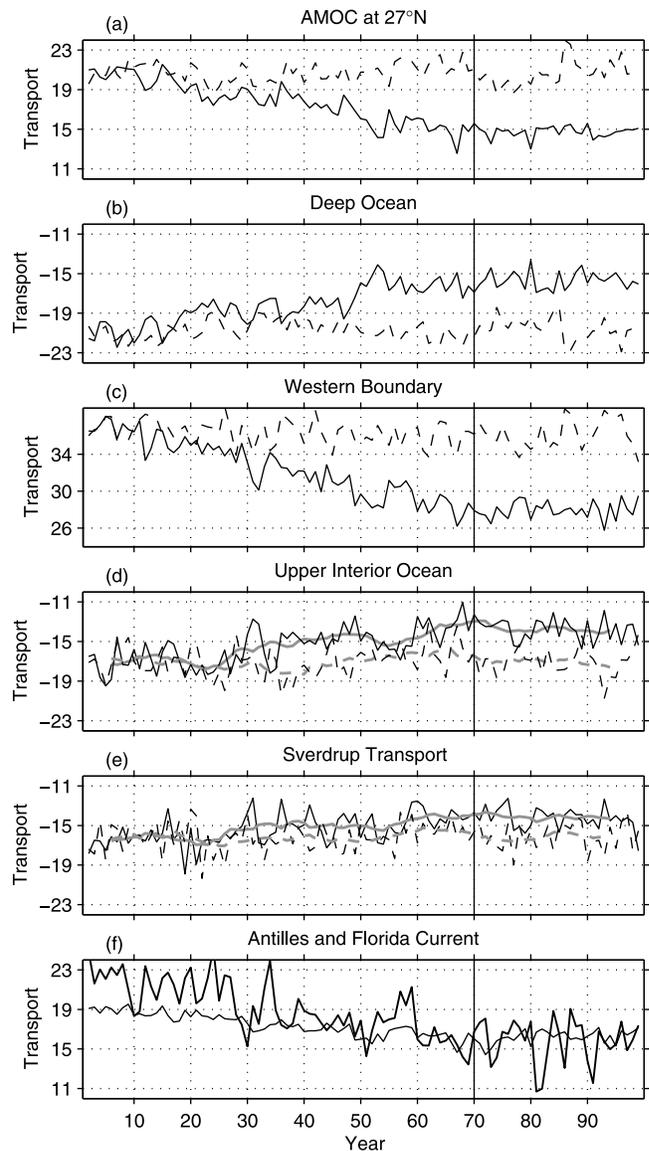

Figure 3. Time series of (a) maximum AMOC at 27°N, (b) transport in the deep ocean, (c) western boundary transport, (d) transport in the upper interior ocean, (e) Sverdrup transport, (f) Florida Current transport (thin line) and Antilles Current transport (bold line) at 27°N. The transports in Figures 3b–3e are zonally integrated and averaged between 17°N and 32°N. Grey lines show smoothing at 10 years. The vertical line marks the year at which CO_2 stops increasing and remains steady. The corresponding dashed lines in 3a–3e are from the Control run. All transports are positive northwards and units are Sverdrups.

of showing only the details of a single latitude (Figure 2c). The southern boundary of the integration region is chosen to lie at 17°N and is approximately at the southern edge of the subtropical gyre. The northern boundary is at 32°N and is where Sverdrup balance errors begin to become large. To calculate the western boundary transport the depth of integration used is the one that encompasses the maximum northward transport and this depth is calculated at each time step. The depth of integration in the interior is kept constant at 1500 m. The southward flowing deep ocean transport is calculated as a basin wide integral over the remaining ocean cross-section. This methodology means it can be ascertained whether changes in the total southwards deep transport are balanced in the northwards boundary current transport or the southwards Sverdrup interior transport.

[15] The southward deep ocean transport reduces by 5.3 Sv during the 70 years of increasing CO_2, before stabilising. The reduction is calculated by subtracting a 30 year mean of the Control from the final 30 years of the 2%CO_2 simulation (Figure 3b). This decrease is large in comparison with the interannual standard deviation of approximately 1.0 Sv in the Control run. The interior ocean transport reduces by 3.4 Sv (compared to an interannual standard deviation of approximately 1.5 Sv). The smoothed time series of interior ocean transport corresponds closely to the time series of Sverdrup transport; the decrease in both is a result of climate change induced weakening of the wind stress curl at subtropical latitudes. The warming climate leads to weaker trade winds and westerlies. A reduction in trade winds appears to be a robust feature of future climate model simulations as a result of a weaker Hadley Cell. However, westerly winds are more commonly shifted polewards than they are weakened [*Lu et al.*, 2008]; only a relatively minor northwards shift takes place here in the 2%CO_2 run [*Catto et al.*, 2011]. Reductions in density that take place over approximately the top 500 m of the subtropical ocean, which are larger on the eastern side than on the western side of the basin (not shown), are consistent with a geostrophic transport reduction in the interior ocean. On scales larger than a few degrees the transport changes are consistent with the wind stress curl changes. Both the temperature and salinity are important in producing the density changes.

[16] The upper ocean western boundary current weakens by 8.7 Sv (compared to 1.3 Sv interannual standard deviation) to compensate for both the 5.3 Sv decrease in deep ocean transport (a weakened AMOC) and the 3.4 Sv decrease in interior upper ocean transport (a weakened subtropical gyre).

[17] In HiGEM, the temperature of water flowing northwards in the western boundary current is similar to the temperature of the southwards interior ocean flow. As a result, the heat transport of the gyre circulation in the North Atlantic is small compared with that of the overturning circulation which involves a large temperature difference between the surface and deep ocean transports. This has been shown in a diagnosis of the horizontal and vertical components of the circulation in HiGEM [*Shaffrey et al.*, 2009] and agrees with ocean observations taken at 26.5°N [*Johns et al.*, 2011]. As a result, the heat transport in the North Atlantic is relatively insensitive to whether a reduction in deep transport is compensated by a reduced upper western boundary current or an increased southward interior flow

because the difference in these scenarios is effectively just a difference in the gyre circulation.

[18] The western boundary domain defined in this study encompasses a portion of the ocean that is commonly included as part of the interior ocean in hydrographic calculations made at 26.5°N [e.g., *Bryden et al.*, 2005; *Kanzow et al.*, 2007]. It is important, however, to remember that the Antilles Current to the east of the Bahamas is a part of the western boundary current system that is not constrained by Sverdrup balance (Figure 1). To understand how the distribution of changes take place within the western boundary region in our model 2%CO_2 simulation at 27°N, we plot time series of the Antilles Current and Florida Current, where these currents are defined as the zonally integrated transport on the east and west sides of the Bahamas at 27°N respectively (Figure 3f).

[19] Both the Florida Current and Antilles Current weaken, with the latter weakening most. The trends in Figure 3f could be misleading because the Antilles Current in HiGEM is too strong relative to observations [*Meinen et al.*, 2004] since it is compensating for a too weak transport through the Florida Straits [*Shaffrey et al.*, 2009]. The results, however, suggest that not all potential changes in the western boundary current will necessarily occur in the Florida Current, and hence in order to gain a full understanding of the structure of AMOC changes in the subtropical ocean, the full western boundary region must be considered.

5. Conclusions

[20] This study has determined how meridional transports in the subtropical North Atlantic re-organize themselves during CO_2 forced climate change in the HiGEM high-resolution coupled climate model. A 5.3 Sv reduction in southward deep transport takes place over 70 years of increasing CO_2 at 2% per year. During the remaining 30 years of the run, when CO_2 levels are held constant, the deep transport remains stable. The main result of this study is that the weakening of the model southwards deep transport is balanced solely by a weakening of the northward upper ocean western boundary current, and not by a strengthening of the interior ocean transport. This is because the zonally integrated interior ocean of HiGEM is in Sverdrup balance throughout the changing climate of the 2%CO_2 scenario (despite the relatively simple assumption that there is always a level of no vertical motion at 1500 m), and because the wind stress curl does not increase. The results suggest that if the AMOC had reduced over the last few decades [*Bryden et al.*, 2005] then the upper ocean change must have occurred in the Antilles Current because no changes have been reported in the Florida Current [*Meinen et al.*, 2010] or wind stress curl [*Atkinson et al.*, 2010].

[21] The model's southward interior ocean transport actually decreases in strength by 3.4 Sv during the 100 years of the 2%CO_2 run. This is the result of a weakened wind stress curl over the interior ocean. The outcome is a western boundary current transport that is further reduced by a total of 8.7 Sv. The decrease in interior ocean transport is a geostrophic transport change consistent with a climate change induced density reduction close to the eastern boundary.

[22] In this study the edge of the western boundary domain has been defined to lie east of all areas where Sverdrup balance breaks down. At 27°N the largest reduction in

western boundary transport in our climate change scenario occurs in the Antilles Current. This suggests that it is important to monitor both of the components of the western boundary system at this latitude since they may contain water masses of different origin and may undergo different changes. This supports earlier findings that show the AMOC is carried mostly through the Florida Straits [*Schmitz and Richardson*, 1991] and the Antilles Current carries most of the gyre return flow [*Lee et al.*, 1996].

[23] The RAPID monitoring system at 26.5°N currently gives daily estimates of the depth structure of the meridional transport integrated across the whole Atlantic basin east of the Bahamas, and is providing valuable insight into the dynamics of AMOC variability. Our results suggest that for the purpose of monitoring change on the decadal time scale that it takes the interior ocean to adjust to Sverdrup balance, one could obtain useful supplementary information from the wind field.

[25] The Editor thanks three anonymous reviewers for their assistance in evaluating this paper.

References

Anderson, D. L. T., and P. D. Killworth (1977), Spin-up of a stratified ocean, with topography, *Deep Sea Res.*, *24*(8), 709–732.

Atkinson, C. P., H. L. Bryden, J. J. M. Hirschi, and T. Kanzow (2010), On the seasonal cycles and variability of Florida Straits, Ekman and Sverdrup transports at 26 degrees N in the Atlantic Ocean, *Ocean Sci.*, *6*(4), 837–859.

Bryden, H. L., H. R. Longworth, and S. A. Cunningham (2005), Slowing of the Atlantic meridional overturning circulation at 25 degrees N, *Nature*, *438*(7068), 655–657.

Catto, J. L., L. C. Shaffrey, and K. I. Hodges (2011), Northern Hemisphere extratropical cyclones in a warming climate in the HiGEM high-resolution climate model, *J. Clim.*, *24*(20), 5336–5352.

Cunningham, S. A., et al. (2007), Temporal variability of the Atlantic meridional overturning circulation at 26.5 degrees N, *Science*, *317*(5840), 935–938.

Gill, A. E. (1982), *Atmosphere–ocean Dynamics*. Academic, San Diego, Calif.

Intergovernmental Panel on Climate Change (2007), *Climate Change 2007: The Physical Science Basis. Contribution of Working Group 1 to the Fourth Assessment Report of the IPCC*, edited by S. Solomon et al., Cambridge Univ. Press, Cambridge, U. K.

Johns, T. C., et al. (2006), The new Hadley Centre climate model (HadGEM1): Evaluation of coupled simulations, *J. Clim.*, *19*(7), 1327–1353.

Johns, W. E., et al. (2011), Continuous, array-based estimates of Atlantic Ocean heat transport at 26.5 degrees N, *J. Clim.*, *24*(10), 2429–2449.

Josey, S. A., E. C. Kent, and P. K. Taylor (2002), Wind stress forcing of the ocean in the SOC climatology: Comparisons with the NCEP-NCAR, ECMWF, UWM/COADS, and Hellerman and Rosenstein datasets, *J. Phys. Oceanogr.*, *32*(7), 1993–2019.

Kanzow, T., et al. (2007), Observed flow compensation associated with the MOC at 26.5 degrees N in the Atlantic, *Science*, *317*(5840), 938–941.

Lee, T. N., W. E. Johns, R. J. Zantopp, and E. R. Fillenbaum (1996), Moored observations of western boundary current variability and thermohaline circulation at 26.5 degrees N in the subtropical North Atlantic, *J. Phys. Oceanogr.*, *26*(6), 962–983.

Lozier, M. S., V. Roussenov, M. S. C. Reed, and R. G. Williams (2010), Opposing decadal changes for the North Atlantic meridional overturning circulation, *Nat. Geosci.*, *3*(10), 728–734.

Lu, J., G. Chen, and D. M. W. Frierson (2008), Response of the zonal mean atmospheric circulation to El Nino versus global warming, *J. Clim.*, *21*(22), 5835–5851.

Meinen, C. S., S. L. Garzoli, W. E. Johns, and M. O. Baringer (2004), Transport variability of the deep western boundary current and the Antilles Current off Abaco island, Bahamas, *Deep Sea Res., Part I*, *51*(11), 1397–1415.

Meinen, C. S., M. O. Baringer, and R. F. Garcia (2010), Florida Current transport variability: An analysis of annual and longer-period signals, *Deep Sea Res., Part I*, *57*(7), 835–846.

Roberts, M. J., et al. (2009), Impact of resolution on the tropical Pacific circulation in a matrix of coupled models, *J. Clim.*, *22*(10), 2541–2556.

Schmitz, W. J., and P. L. Richardson (1991), On the sources of the Florida Current, *Deep Sea Res., Part A*, *38*, S379–S409.

Searl, Y., H. T. Banks, S. Stark, and R. A. Wood (2007), Slowing of the Atlantic meridional overturning circulation: A climate model perspective, *Geophys. Res. Lett.*, *34*, L03610, doi:10.1029/2006GL028504.

Shaffrey, L. C., et al. (2009), UK HiGEM: The new UK high-resolution global environment model-model description and basic evaluation, *J. Clim.*, *22*(8), 1861–1896.

Sverdrup, H. U. (1947), Wind-driven currents in a baroclinic ocean—With application to the equatorial currents of the eastern Pacific, *Proc. Natl. Acad. Sci. U. S. A.*, *33*(11), 318–326.

Wunsch, C. (2011), The decadal mean ocean circulation and Sverdrup balance, *J. Mar. Res.*, *69*(2–3), 417–434.

Wunsch, C., and P. Heimbach (2006), Estimated decadal changes in the North Atlantic meridional overturning circulation and heat flux 1993–2004, *J. Phys. Oceanogr.*, *36*(11), 2012–2024.